Disorder and de-coherence in graphene probed by low-temperature magneto-transport: weak localization and weak antilocalization

2013 J. Phys.: Conf. Ser. 456 012032

(http://iopscience.iop.org/1742-6596/456/1/012032)

Journal of Physics: Conference Series **456** (2013) 012032 doi:10.1088/1742-6596/456/1/012032

Disorder and de-coherence in graphene probed by low-temperature magneto-transport: weak localization and weak antilocalization

S.Pezzini[1,2], C.Cobaleda[2], E.Diez[2] and V.Bellani[1]

[1] Dipartimento di Fisica and CNISM, Università degli studi di Pavia, I-27100 Pavia, Italy
[2] Laboratorio de Bajas Temperaturas, Universidad de Salamanca, E-37008 Salamanca, Spain

E-mail: sergio.pezzini@unipv.it

Abstract. We studied weak localization (WL) and and weak antilocalization (WAL) in a eight-contacts Hall bar made of exfoliated monolayer graphene on Si-SiO_2, by means of magneto-transport experiments, at temperatures between 0.3 K and 15 K. At low carrier density ($n \simeq 7 \times 10^{11}\ cm^{-2}$) we observed a transition from WL to WAL driven by the increasing of the magnetic field, while at high carrier density ($n \simeq 2 \times 10^{12}\ cm^{-2}$) only WL was observable. We analyzed the magnetic field driven WL-WAL transition and we evaluated the temperature dependence of the de-coherence parameters using an alternative method compared to previous studies. The values we obtained were corroborated by a root-mean-square analysis of the amplitude of highly-reproducible universal conductance fluctuations.

1. Introduction

The two-dimensional material graphene represents one of the most intriguing systems in present-day condensed-matter physics [1, 2]. Among its numerous outstanding properties, the relativistic behavior of chiral charges in graphene can be considered the most prominent [3, 4, 5]. The charge carriers are indeed governed by the Dirac-like Hamiltonian $H_{\mathbf{K}} = v_f \boldsymbol{\sigma} \cdot \mathbf{p}$ (where $v_f \simeq 10^6\ \frac{m}{s}$ is the Fermi velocity of electrons in graphene, $\mathbf{p}$ is the momentum operator and $\boldsymbol{\sigma}$ the *pseudospin* operator) in the proximity of the so-called Dirac points **K** and **K'**, two classes of special points in the reciprocal space, placed at the vertexes of the hexagonal first Brillouin zone. The eigenvalues $E_{\pm} = \pm v_f \hbar |\mathbf{q}|$ describe a linear energy-momentum dispersion, with degeneracy at the Dirac points. The eigenstates of $H_{\mathbf{K}}$ are two-components spinors and simultaneous eigenstates of the helicity operator $h = \boldsymbol{\sigma} \cdot \mathbf{p}/|\mathbf{p}|$,with positive or negative eigenvalues depending on the relative orientation of momentum and pseudospin: $+1$ for electrons in **K** valley (holes in **K'** valley), -1 for electrons at **K'** (holes at **K**) (see Fig. 1(a)). In addition, as a consequence of the topology of the energy bands, a non-trivial Berry phase $\gamma = \pi$, is associated with those states (i.e. they change their sign when covering a closed circuit in reciprocal space including **K** or **K'**).

Chirality and Berry phase are especially crucial when coherent backscattering events in graphene are considered. In case of *intravalley* events (black arrow in Fig. 1(a)), the conservation of the helicity eigenvalue forbids backscattering, namely the chiral charges are expected to perform the so-called *Klein tunneling* paradox [6, 7]. On the other hand, backscattering is

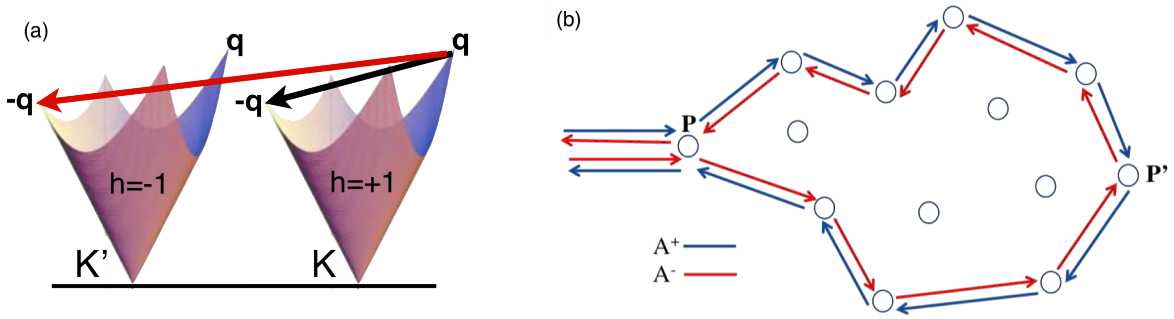

Figure 1: (a) Pictorial view of graphene's conduction band at K and K', with sketched intravalley (black arrow) and intervalley (red arrow) backscattering events. (b) Schematic picture of two closed PP'P electronic paths. A probability amplitude $A^+ = ae^{i\varphi^+}$ ($A^- = ae^{i\varphi^-}$) is associated to the clockwise (counterclockwise) trajectory, giving a backscattering probability $p = |A^+ + A^-|^2 = 2a^2(1 + \cos(\varphi^+ - \varphi^-))$.

allowed for *intervalley* events (black arrow in Fig. 1(a)), as the change of sign of the momentum is accompanied by a change of sign in helicity.

From a complementary point of view, the quantum interference between time-reversed counter-propagating closed electronic paths (for instance the two trajectories sketched in Fig. 1(b)) has to be taken into account. Depending on the phase difference acquired by the charge carrier while covering the two paths, constructive or destructive interference can occur. In the first case the backscattering probability is enhanced, so that the electrical conductivity is lowered with respect to the standard Drude's σ_0 [8], i.e. weak localization (WL) takes place [9, 10]. In the second case the backscattering probability is lowered, then the electrical conductivity is increased with respect to σ_0, i.e. one observes weak antilocalization (WAL). The π Berry phase implies destructive interference (and therefore WAL) for intravalley events, while produces constructive interference (and then WL) for intervalley ones. As a consequence, both WL and WAL can occur in graphene, their grade and presence depending on different types of elastic scattering mechanisms. Long-range potentials (such as ripples, dislocations and charged impurities) are responsible for intravalley events, while short-range potentials (adatoms, vacancies) induces intervalley ones.

The study of the WL-WAL corrections to conductivity in a graphene sample can therefore provide significant information about the disorder affecting the sample itself. A mean scattering time τ_s can be associated to intravalley events, while τ_i is the analogous for intervalley ones. Nevertheless, another contribution to intravalley scattering τ_w has to be taken into account, for the trigonal warping of the energy bands far from the Dirac points restores some backscattering probability as helicity ceases to be a good quantum number. Accordingly, the WL-WAL behavior experimentally observable depends on the relative incidence of these parameters.

Quantum interference corrections are suppressed by the breaking of time-reversal symmetry and the loss of phase coherence of charge carriers. Time-reversal can be broken by applying a non-zero magnetic field perpendicular to the graphene plane, which sets an upper time limit $\tau_B \propto B^{-1}$ to the the scatterings contributing to WL and WAL. Accordingly, WL manifests as a conductivity increasing with the magnetic field, while WAL corresponds to a decreasing magneto-conductivity. Decoherence due to inelastic scatterings is taken into account by introducing a characteristic time-scale (length-scale) parameter τ_ϕ (l_ϕ), that competes with the above mentioned scattering times in determining the quantum interference corrections to conductivity.

A complete expression for the magneto-conductivity in graphene, which embodies all the

described effects, has been derived by E. McCan *et al.* in 2006 [11]; the analysis of the experimental data is usually based on the use of such function [12, 13, 14]. Nevertheless, we will try to follow a more intuitive procedure hereafter. We will not perform a fit of our data, we will rather make use of approximated relations in order to relate the WL-WAL magneto-conductivity to the mean elastic and inelastic scattering rates, at different carrier densities and temperatures.

2. Measurements and data analysis

We studied the electrical transport properties of an eight-contacts Hall bar made of mechanically exfoliated graphene, placed on a standard Si/SiO_2 (300 nm thick) substrate, with dimension $W \times L = 5.1\ \mu m \times 10.6\ \mu m$ (corresponding to a geometrical factor $W/L \simeq 0.5$). The longitudinal and Hall measurements were performed with standard low-frequency (10 Hz $< f <$ 15 Hz) ac lock-in technique, forcing a current of intensity 1 nA $< I <$ 10 nA to flow across the graphene. The sample was placed in a cryogen-free ^{3}He refrigerator with base temperature $\simeq 0.3$ K, located in a cryogen-free superconducting magnet.

As a preliminary step, we performed measurements of longitudinal resistivity as a function of back-gate voltage at zero magnetic field and $T = 0.3$ K, reconstructing the so-called Dirac peak of the sample (Fig. 2(a)). Following the fit procedure developed by Kim *et al.* [15], we estimated the charge neutrality point at $V_D \simeq 4.66$ V, with a residual charge density $n_{res} \simeq 2 \times 10^{11}\ cm^{-2}$. A chearged impurities' concentration at SiO_2-graphene interface $n_{imp} \simeq 10^{12}\ cm^{-2}$ was estimated making use of the relation $n_{res} \simeq 0.2 \times n_{imp}$ [16]. The average separation between such impurities resulted therefore $l_{imp} \simeq 10\ nm$, two order of magnitude larger than the nearest-neighbor distance $a = 1.42\ \mathring{A}$, thus satisfying the condition $l_{imp} \gg a$. The slowly-varying long-range potential associated with the charges randomly-located below the graphene plane can result in a finite electrostatic gradient inside the unit cell (i.e. an asymmetry between the two sublattices), which has been shown to produce an effective breaking of time-reversal symmetry (and therefore sets a temporal cutoff to the interference events) [17].

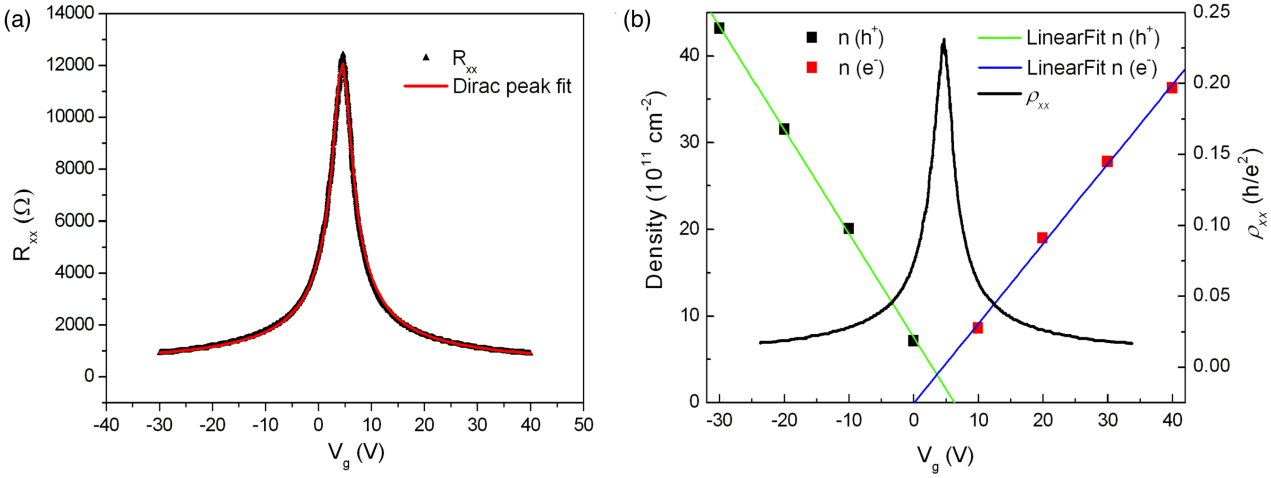

Figure 2: (a) Field effect in graphene: Dirac peak of the sample, fitted with the function of Kim *et al.* [15]. (b) Two dimensional density of carriers and resistivity as a function of gate voltage.

The two dimensional density of charge carriers (n, see Fig. 2(b)) was estimated both in the hole and electron regime at $T = 0.3$ K, from the Hall resistance (R_{xy}) measurements, making use of the relation n=$1/(es)$ (where $s = dR_{xy}/dB$ was obtained form a linear fit of $R_{xy}(B)$). The Hall mobility $\mu = 1/(ne\rho^0_{xx})$ (where ρ^0_{xx} is the longitudinal resistivity at $B = 0$ T) was also evaluated and resulted $\mu \sim 4 \times 10^3\ cm^2V^{-1}s^{-1}$ at carrier density $n \simeq 7 \times 10^{11}\ cm^{-2}$. A slight decrease of

the mobility was found as a consequence of the increase of the carrier density (e.g. $\mu \sim 3.6 \times 10^3$ $cm^2V^{-1}s^{-1}$ at $n \simeq 2 \times 10^{12}$ cm^{-2})).

We successively performed measurements of the magneto-conductivity at different gate voltages (in the hole regime) and temperatures (between 0.3 K and 15 K), in order to determine the evolution of the quantum-interference corrections. The most significant data are shown in Fig. 3.

At very low field all the curves present a deep minimum at $B = 0$ T and a subsequent increasing magneto-conductivity, indicating WL behavior. At $V_g = 0$ V (corresponding to $n \simeq 7 \times 10^{11}$ cm^{-2}, see Fig. 3(a)) the magneto-conductivity curves reach a maximum at $B \simeq 0.06$ T (which is independent from temperature) and decrease at higher field: a B-driven transition from WL to WAL occurs. Such transition is expected to take place at a characteristic magnetic field B_i at which $\tau_B \approx \tau_i$ [11]. However, in order to take into account the field dependence of the WL correction (given by the function presented in Ref. 11), such value must be renormalized by a factor $4e^{\gamma}$ (where γ is the Euler-Mascheroni constant). From the renormalized value of B_i, we estimated for our sample a mean intervalley scattering rate $\tau_i^{-1} \simeq 0.5 \times 10^{12}$ s^{-1} at low carrier density. The fact that WAL is observable for $B > B_i$ (i.e. WAL "survives" at much smaller τ_B) indicates that intravalley scatterings take place at lower time-scale with respect to intervalley events; we can therefore argue that $\tau_s^{-1} \gg \tau_i^{-1}$, namely that the intravalley long-range scattering centers (such as charged impurities) dominate over short-range intervalley ones in our sample.

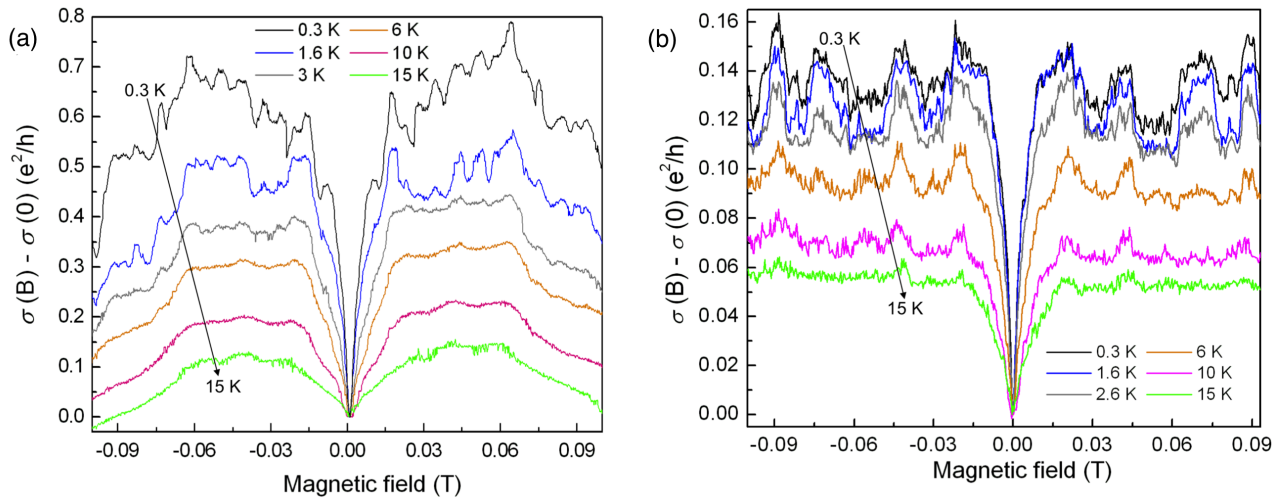

Figure 3: Evolution with temperature of magneto-conductivity, for $V_g = 0$ V (a) and $V_g = -10$ V (b).

The data collected at $V_g = -10$ V ($n \simeq 2 \times 10^{12}$ cm^{-2}, see Fig. 3(b)), on the other hand, does not show evidence of WAL. The applied gate potential sets the Fermi level far from the Dirac points, where the trigonal warping suppresses the chirality conservation and, accordingly, the WAL effect. Therefore, passing from $V_g = 0$ V to $V_g = -10$ V the sample is switched from a regime where $\tau_s^{-1} > \tau_w^{-1}$ to a trigonal warping-dominated regime, where $\tau_s^{-1} < \tau_w^{-1}$. Also for these data, a characteristic magnetic field B_i (at which $\tau_B \approx \tau_i$) marks the suppression of WL. We estimated $B_i \simeq 0.02$ T (for $B > B_i$ only fluctuations are observable), which gives, after proper renormalization with the factor $4e^{\gamma}$, $\tau_i^{-1} \simeq 0.3 \times 10^{12}$ s^{-1}. We believe that the intervalley scattering rate is lowered as a consequence of the increasing of Coulomb screening on the short-range scatterers for $n = 2 \times 10^{12}$ cm^{-2}.

After evaluating the relative strength of the different elastic mechanisms, we centered on the de-coherence of charge carriers. Considering that in graphene only intervalley scattering processes contribute to WL, we approximated of the function of Ref. 11 in order to obtain a

simple analytical expression relating the amplitude of the WL correction to the de-coherence time

$$\delta\sigma^{WL}(\frac{e^2}{h}) = \frac{1}{\pi}\ln(1+2\frac{\tau_\phi}{\tau_i}) \quad (1)$$

Making use of Eq. 1 we could easily estimate the de-coherence parameters from the peak-to-valley value of the WL conductivity dips of Fig. 3 and the mean intervalley scattering time. In Fig. 4(a) we can see that the phase-breaking rate τ_ϕ^{-1} grows linearly with temperature and that in the high density regime it has larger values (and increases more rapidly) then in the low density regime. The linear dependence of τ_ϕ^{-1} indicates that the carrier-carrier Coulomb interaction is the dominant de-phasing mechanism, in accordance with previous studies [12].

A finite offset is clearly observable in the de-phasing rate at high carrier density, indicating the presence of some other mechanisms competing with e-e de-coherence in determining the temporal cutoff to the interference processes at low temperature. A possible explanation can be found taking into account the effective breaking of time-reversal symmetry induced by the charged impurities at the graphene-SiO_2 interface [17]. This effect is expected to be relevant in case of decoupling of the **K** and **K'** valleys, namely for low intervalley scattering rate, which is the case of our high-density regime at $V_g = -10$ V. This mechanism can be mapped into the presence of an effective magnetic field, resulting into a suppression of the WL amplitude at low temperature: from the saturation value $\tau_\phi^{-1} \simeq 0.75 \times 10^{12}\ s^{-1}$ (obtained by a linear fit, see Fig. 4(a)), we estimated $B_{eff} \simeq 8$ mT.

A root-mean-square analysis of the magnitude of highly-reproducible universal conductance fluctuations (UCF, see Fig. 4(b)), based on the methodology of of P. A. Lee *et al.* [18], gave us a confirmation of the reliability of the values of Fig. 4(a). The analysis was performed considering the magneto-conductivity in the range 0.03 T $< B <$ 0.06 T for the V_g= 0 V case and the range 0.03 T $< B <$ 0.09 T for $V_g = -10$ V (i.e. the ranges where the UCF are well resolved). The extracted de-phasing rates at $T = 0.3$ K, $\tau_\phi^{-1}(V_g$=0 V$) \simeq 0.16 \times 10^{12}\ s^{-1}$ (orange triangle in Fig. 4(a)) and $\tau_\phi^{-1}(V_g$=-10 V$) \simeq 0.97 \times 10^{12}\ s^{-1}$ (orange square), are in a very satisfying agreement with the values obtained from Eq. 1.

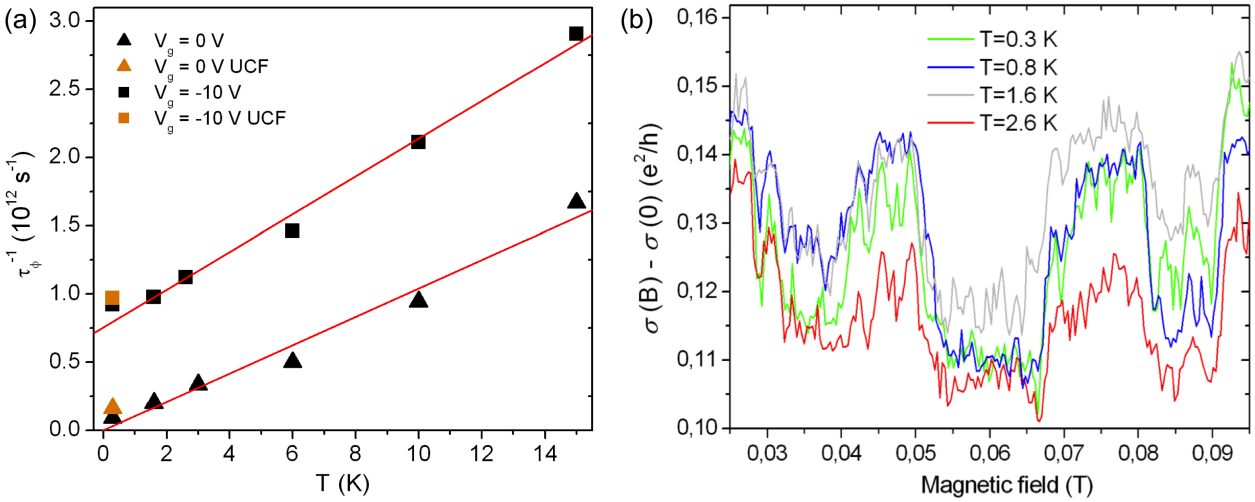

Figure 4: (a) De-coherence length and rate as a function of temperature both for $V_g = 0$ V and $V_g = -10$ V. (b) Universal conductance fluctuations measured at $T \leq 3$ K for $V_g = -10$ V.

3. Conclusions

In conclusion, we studied the quantum interference corrections to magneto-conductivity in mechanically exfoliated monolayer graphene at different charge carrier densities in the hole region. We found evidence of both WL or WL combined with WAL depending on the relative strength of the various elastic scattering mechanisms. The temperature dependence of de-coherence rate has been estimated using a simplified method with respect to previous studies, and indicates that the carrier-carrier Coulomb interaction is the main de-phasing mechanism in graphene at our densities. The low-temperature saturation of the de-coherence rate in the high carrier density regime can be related to an effective breaking of time-reversal symmetry due to the presence of long-range slowly-varying potentials, that have been shown to be the dominant disorder. The extreme sensitivity of WL-WAL to various elastic scattering mechanisms hints the use of magneto-transport measurements as a tool of characterization of both unintentional and intentional disorder in graphene.

Acknowledgements

We are thankful to David López and Mario Amado and to the ISOM for their help during the sample process. This work has been supported by the following projects: MICINN (Spain) FIS2009-07880 and PCT310000-2009-3 and Junta de Castilla y León SA049A10.

References

[1] K. S. Novoselov, A. K. Geim, S. V. Morozov, D. Jiang, Y. Zhang, S. V. Dubonos, I. V. Grigorieva and A. A. Firsov, Science **306**, 666 (2004).
[2] K. S. Novoselov, A. K. Geim, S. V. Morozov, D. Jiang, M. I. Katsnelson, I. V. Grigorieva, S. V. Dubonos, and A. A. Firsov, Nature **438**, 197 (2005).
[3] K. S. Novoselov, S. V. Morozov, T. M. G. Mohiuddin, L. A. Ponomarenko, D. C. Elias, R. Yang, I. I. Barbolina, P. Blake, T. J. Booth, D. Jiang, J. Giesbers, E. W. Hill, and A. K. Geim, Phys. Stat. Sol. (b) **244**, 4106 (2007).
[4] A. H. Castro Neto, F. Guinea, N. M. R. Peres, K. S. Novoselov, and A. K. Geim, Rev. Mod. Phys. **81**, 109 (2009).
[5] R. N. M. Peres, Rev. Mod. Phys. **82**, 2673 (2010).
[6] O. Klein, Z. Phys. **53**,157 (1929).
[7] M. I. Katsnelson, K. S. Novoselov, and A. K. Geim, Nature Physics **2**, 620 (2006).
[8] N. W. Ashcroft and N. D. Mermin, Solid State Physics, Holt, Rinehart and Winston, New York (1976).
[9] C. W. J. Beenakker and H. van Houten, Solid State Phys. **44**, 1 (1991).
[10] G. Bergmann, Phys. Rev. B **28**, 2914 (1983).
[11] E. McCann, K. Kechedzhi, V. I. Fal'ko, H. Suzuura, T. Ando, B. L. Altshuler, Phys. Rev. Lett. **97**, 146805 (2006).
[12] S. V. Morozov, K. S. Novoselov, M. I. Katsnelson, F. Schedin, L. A. Ponomarenko, D. Jiang, and A. K. Geim, Phys. Rev. Lett. **97**, 016801 (2006).
[13] F. V. Tikhonenko, D. W. Horsell, R. V. Gorbachev, and A. K. Savchenko, Phys. Rev. Lett. **100**, 056802 (2008).
[14] F. V. Tikhonenko, A. A. Kozikov, A. K. Savchenko, and R. V. Gorbachev, Phys. Rev. Lett. **103**, 226801 (2009).
[15] S. Kim, J. Na, I. Jo, D. Shahrjerdi, L. Colombo, Z. Yao, E. Tutuc, and S. K. Banerjee, Appl. Phys. Lett. **94**, 062107 (2009).
[16] S. Adam, E. H. Hwang, V. M. Galitski, and S. Das Sarma, Proc. Natl. Acad. Sci. U.S.A. **104**, 18392 (2007).
[17] A. F. Morpurgo and F. Guinea, Phys. Rev. Lett. **97**, 196804 (2006).
[18] P. A. Lee, A. D. Stone and H. Fukuyama, Phys. Rev. B **35**, 1039 (1987).